Structure of domain walls in an oscillator array

Joseph Rudnick
Department of Physics, University of California at Los Angeles, 405 Hilgard Avenue, Los Angeles, California 90024-1547
(Received 25 October 1993)

An array of parametrically driven pendulums has been found to exhibit a remarkably wide range of behavior. Here, we establish an analytically based model for a type of domain wall that is, so far, unique to this system. This domain wall separates two regions in containing standing wave modes having different wavelengths. The model entails the "elimination" of a fraction of the oscillators. Numerical predictions based on this model are compared with data generated by numerically solving the equations of motion of a one-dimensional lattice of coupled nonlinear oscillators. The agreement between theory and numerical simulation is, by and large, satisfactory.

PACS number(s): 03.20.+i, 46.10.+z, 63.20.Pw, 63.20.Ry

I. INTRODUCTION

Ever since the observation of a galaxy of subharmonics in the gravity waves on the surface of a long, narrow trough of water [1], and the subsequent discovery of a nonpropagating solitary wave in the same configuration [2], experimental studies of this hydrodynamical system and its discrete analog, a parametrically excited array of coupled pendulums, have generated new and interesting dynamical effects [3,4]. This paper is about two recently observed domain-wall-like structures appearing in the one-dimensional lattice of coupled pendulum [3]. These spatially localized configurations represent variations on the nonpropagating soliton described above. As will be demonstrated, there are cases in which the domain wall in the pendulum lattice differs from the hydrodynamic soliton in that its existence appears to demand an underlying system that is spatially resolvable into discrete components. This is true for one of the types of domain walls discussed in this paper, and we must modify the approaches previously taken in the study of nonpropagating solitons.

The behavior of domain walls in the context of condensed-matter physics dominates many important phenomena, including, but not limited to, phase coexistence in systems with a broken discrete symmetry. The idea that domain walls can be understood as localized structures in a continuous system governed by nonlinear differential equations dates back to the work of van der Waals on the gas-liquid interface near a critical point [5]. In addition, some of the most interesting solitary wave solutions in integrable systems possess a domain-wall-like structure, such as the kink in the sine-Gordon equation [6].

A characteristic of the domain wall on which attention is focused in this paper is that it seems to owe its existence to the inherently discrete nature of the system that supports it. Given this, one hopes that the investigation on which we report here will lead to a deeper understanding of the physics and mathematics of domain walls.

Denardo *et al.* [7] develop an alternative approach to the kind of domain wall upon which we focus our attention in this paper. Their model is a continuous one, and they discuss the dynamical steady states of their system in terms of a sinusoidal displacement function with an amplitude and effective wavelength that have slow spatial variations. This approach leads to equations for a domain wall separating two regions having different asymptotic wavelengths. The solution holds only when a certain global criterion is met. In the case of the pendulum lattice, this condition is found not to hold.

The focus of the investigation undertaken here is the set of steady-state solutions of the equations of motion of the pendulum lattice. However, in the steps leading to the equations governing fixed-amplitude oscillations we allow for the possibility of configurations that evolve in time. Thus, one ought to be able to adapt the method utilized here to study the chaotic motion that has recently been observed to occur in a domain wall [4].

Following is an outline of the paper. In Sec. II, we will develop the equations of motion of a lattice of coupled pendulums in terms of the evolution in time of their amplitudes and phase angles, under the assumption that the temporal scale for this evolution is large compared to the natural periods of the pendulums' oscillations. The pendulums are subject to damping forces and are driven parametrically. The ultimate result of this section is a set of equations for their steady-state amplitudes. These equations are discrete analogs of the equations that gave rise to the amplitudes of the nonpropagating hydrodynamic soliton. In particular, they constitute the discrete version of the nonlinear Schrödinger equation. Section III contains a description of the domain walls of interest. The first and simplest type separates two regions in which the "upper cutoff" mode oscillates stably. It can be described in terms of a phase slip. Viewed this way, the domain wall, previously modeled with the use of a nonlinear Schrödinger equation [7], is now described by a solution of the sine-Gordon equation. In Sec. IV an alternative approach to the study of the phase-slip domain wall is developed. This approach involves a reduction of the equations governing the amplitudes of oscillator amplitudes so that it applies to every other oscillator. We find that the solution for the domain wall can depart

significantly from the sine-Gordon, or nonlinear Schrödinger equation, kink.

Section V extends the method described in Sec. IV so that it applies to the domain wall separating modes having different wavelengths. In particular, we consider the case of an "upper cutoff" mode, having a wavelength equal to twice the distance between oscillators and a "midband" mode, the wavelength of which is four times the interoscillator distance. When the equations describe the steady-state motion of every *fourth* oscillator a version of the slowly-varying-envelope approximation applies. In Sec. VI numerical results for the shape of the domain wall, obtained by integrating the equation developed in Sec. V, are compared with the results of a simulation of the motion of the one-dimensional oscillator array. Agreement is generally satisfactory. Section VII contains some concluding comments, including a discussion of the genesis of the global condition of Denardo, *et al.* [7]. It is hoped that the method described in Secs. V and VI of this paper can be applied to phenomena other than the domain walls discussed here.

II. EQUATIONS OF MOTION

The pendulum lattice consists of a set of coupled nonlinear oscillators. The nonlinearity is due to the dependence on displacement from the vertical of the torque exerted by the gravitational field. If the displacement of the ith pendulum in the lattice is denoted by $x_i(t)$, then the equation of motion of that pendulum has the form

$$\frac{d^2x_i}{dt}+\gamma\frac{dx_i}{dt}+k_1x_i+k_2(2x_i-x_{i-1}-x_{i+1})-\alpha x_i^3 = Fx_i\cos(\Omega t)\ . \quad (2.1)$$

The nonlinear term αx_i^3 represents the softening of the gravitational restoring force as the pendulum departs from the vertical.

As a first step in the development of the approximations that constitute the foundation of our analysis we express the variable x_i as in terms of an amplitude and a phase angle, as follows:

$$x_i(t)=A_i(t)\sin\left[\frac{\Omega}{2}t+\phi_i(t)\right]\ , \quad (2.2)$$

then

$$y_i(t)\equiv\frac{dx_i}{dt}\approx\frac{\Omega}{2}A_i(t)\cos\left[\frac{\Omega}{2}t+\phi_i(t)\right]\ . \quad (2.3)$$

The approximate equality above is based on the assumption that the time derivative of the phase factor $\phi_i(t)$ is small compared to the frequency, Ω, of the parametric modulation.

With the use of the definition in Eq. (2.3) we reduce the equation of motion (2.1) to the two following first-order differential equations

$$\frac{dx_i}{dt}=y_i \quad (2.4)$$

and

$$\frac{dy_i}{dt}=-\gamma y_i-k_1x_i-k_2(2x_i-x_{i+1}-x_{i-1})+\alpha x_i^3+Fx_i\cos(\Omega t)\ . \quad (2.5)$$

Equations for the time evolution of the amplitudes and phases are obtained as follows: Multiplying Eq. (2.4) by $x_i(t)$ and Eq. (2.5) by $(2/\Omega)^2y_i(t)$ and adding

$$x_i\frac{dx_i}{dt}+\left[\frac{2}{\Omega}\right]^2y_i\frac{dy_i}{dt}=\frac{1}{2}\frac{d}{dt}\left[x_i^2+\left[\frac{2}{\Omega}\right]^2y_i^2\right]=\frac{1}{2}\frac{dA_i^2}{dt}=x_iy_i+\left[\frac{2}{\Omega}\right]^2[-\gamma y_i^2-k_1x_iy_i-k_2y_i(2x_i-x_{i+1}-x_{i-1})+\alpha x_i^3y_i+Fx_iy_i\cos(\Omega t)]\ . \quad (2.6)$$

We then express the variables $x_i(t)$ and $y_i(t)$ in terms of the amplitudes and phases with the use of Eqs. (2.2) and (2.3) and average the resulting equations over a cycle of the drive, assuming that $A_i(t)$ and $\phi_i(t)$ remain constant. The terms on the right-hand side of Eq. (2.6) that survive the averaging process yield the following equation for the time development of the amplitude A_i:

$$\frac{1}{2}\frac{dA_i^2}{dt}=-\frac{\gamma}{2}A_i^2+\frac{F}{4}\left[\frac{2}{\Omega}\right]A_i^2\sin(2\phi_i(t))\ . \quad (2.7)$$

The equation governing the time development of the phase angle $\phi_i(t)$ is obtained by making use of the relationship

$$\phi_i=\arctan\left[\frac{x_i}{y_i}\times\frac{\Omega}{2}\right]-\frac{\Omega}{2}t\ , \quad (2.8)$$

so

$$\frac{d\phi_i}{dt}=\frac{\left[\frac{2}{\Omega}\right]\left[y_i\frac{dx_i}{dt}-x_i\frac{dy_i}{dt}\right]}{x_i^2+\left[\frac{2}{\Omega}\right]^2 y_i^2}-\frac{\Omega}{2} . \tag{2.9}$$

Replacing $x_i(t)$ and $y_i(t)$ by the right-hand sides of Eqs. (2.2) and (2.3), and time averaging as above, we obtain the equation of motion

$$A_i\frac{d\phi_i}{dt}=\frac{2}{\Omega}\left[\frac{A_i}{2}\left[\frac{\Omega}{2}\right]^2+\frac{k_1 A_i}{2}+\frac{k_2}{2}[2A_i-A_{i-1}-A_{i+1}]-\alpha A_i^3\right]+\frac{A_i F}{4}\left[\frac{2}{\Omega}\right]\cos(2\phi_i)-\frac{\Omega}{2}A_j . \tag{2.10}$$

Equations (2.7) and (2.10) are the basis of all the analysis that follows.

III. STEADY-STATE SOLUTIONS: NONPROPAGATING SOLITON AND SIMPLE DOMAIN WALL

If the lattice has settled into a steady state, all pendulums oscillating with half the frequency of the parametric drive, the amplitudes, $A_i(t)$, and the phase angles, $\phi_i(t)$, are constant in time. Then, from Eq. (2.7),

$$\frac{F}{4}\frac{2}{\Omega}\sin(2\phi_i)=\frac{\gamma}{2} . \tag{3.1}$$

Notice that the existence of a solution to the above equation implies the inequality $F>\gamma\Omega$. As in all other cases, parametric excitation of the pendulum lattice is a threshold phenomenon. The equations that follow from Eqs. (2.10) when the lattice has achieved a dynamically steady state are

$$0=\frac{2}{\Omega}\left[\frac{A_i}{2}\left[\frac{\Omega}{2}\right]^2+\frac{k_1 A_i}{2}+\frac{k_2}{2}[2A_i-A_{i-1}-A_{i+1}]-\alpha A_i^3\right]-\frac{\Omega}{2}A_i+A_i\left[\left[\frac{F}{4}\frac{2}{\Omega}\right]^2-\frac{\gamma^2}{4}\right]^{1/2} . \tag{3.2}$$

In the above equation we have utilized Eq. (3.1) to express $\cos(2\phi_i)$ in terms of other parameters.

To simplify the notation we note that Eq. (3.2) can be written as follows:

$$aA_i-b(A_{i+1}+A_{i-1})-cA_i^3=0 , \tag{3.3}$$

where

$$a=-\frac{\Omega}{4}+\frac{k_1}{\Omega}+\frac{2k_2}{\Omega}+\left[\left[\frac{F}{4}\frac{2}{\Omega}\right]^2-\frac{\gamma^2}{4}\right]^{1/2} , \tag{3.4}$$

$$b=\frac{k_2}{\Omega} , \tag{3.5}$$

$$c=\frac{2\alpha}{\Omega} . \tag{3.6}$$

While the coefficient a has a sign that depends on adjustable parameters, the signs of coefficients b and c are fixed and positive.

Equation (3.3) is a discrete version of the nonlinear Schrödinger equation. If we set the nominal spacing between the pendulums equal to one, and assume that the amplitudes vary slowly as the lattice index is changed, then Eq. (3.3) can be approximated as follows:

$$(a-2b)A(z)-b\frac{d^2A(z)}{dz^2}-cA(z)^3=0 , \tag{3.7}$$

where the discrete index i has been replaced by the continuous variable z. This equation supports the following localized solution

$$A(z)=\left[\frac{2(a-2b)}{c}\right]^{1/2}\operatorname{sech}\left[\left[\frac{b}{a-2b}\right]^{1/2}(z-z_0)\right] , \tag{3.8}$$

which is the nonpropagating soliton, first seen in a trough of water [1], and subsequently observed in a pendulum lattice [2].

The discrete equation also supports extended solutions. If we neglect the nonlinear term and $a-2b<0$, then solutions of the form $A_i\propto\sin(ki)$ follow, where $k^2=(2b-a)/b$. If the nonlinear coefficient c is small, the actual solutions are, in general, close to the sinusoidal solution. A detailed analysis of the stability of the extended solutions requires application of the types of techniques that have been used to study systems exhibiting Kolmogorov-Arnold-Moser–type behavior [8].

In fact, Eq. (3.3) represents an example of the kind or area-preserving map to which a good deal of attention is still being paid. If we define $\Delta_i\equiv A_i-A_{i-1}$, then the equation can be replaced by the following set of recursion relations

$$A_{i+1}=A_i+\Delta_{i+1} , \tag{3.9}$$

$$\Delta_{i+1}=\Delta_i+\frac{a-2b}{b}A_i-\frac{c}{b}A_i^3 . \tag{3.10}$$

This map gives rise to periodic and fixed-point behavior, and to "Hamiltonian chaos." There is the intriguing possibility that the pendulum lattice provides a spatial arena for the observation of the kind of temporal behavior that continues to excite the interest of scientists and mathematicians.

In addition, the recursion relations above have relevance to the mean-field theory of charge-density waves [9]. This relationship, which deserves further study, will not be pursued here.

The crux of the investigation reported here is a domain wall separating two *particular* periodic solutions to the discrete steady-state equations. These two solutions are, first the "upper cutoff" mode in which amplitudes alternate as follow: $A_k=(-1)^k A_0$, and, second, the "midband" mode in which the amplitude repeats itself every four sites. The explicit structure of this mode is

$A_{2K}=(-1)^k A_1$, $A_{2k+1}=0$. In both cases the nonzero amplitudes are found—with no great difficulty—by substituting the solutions into Eq. (3.3). One finds

$$A_0=\sqrt{a+2b/c}\ , \tag{3.11}$$

and

$$A_1=\sqrt{a/c}\ . \tag{3.12}$$

It is immediately clear that certain requirements must be met in order for the modes in question to exist. In particular, the pendulum lattice supports the upper cutoff mode only if $a+2b>0$, while dynamical stability of the midband mode requires $a>0$.

Assuming that the first inequality is satisfied and, furthermore, that the system is just past the threshold of dynamical stability of the upper cutoff mode ($a+2b$ is positive and small), we can construct a continuous approximation to the equations governing the domain wall separating two regions in which this mode is supported. The domain wall defines a region in which there is a localized phase slip. We will cast the description of the domain wall in a form that clearly exhibits this phenomenon. We do this by writing

$$A_k=A_0\cos(k\pi+\delta_k)\ . \tag{3.13}$$

Equation (3.3) becomes

$$A_0[a\cos\delta_k+b(\cos\delta_{k+1}+\cos\delta_{k-1})] -cA_0^3(\cos\delta_k)^3=0\ . \tag{3.14}$$

If we assume that the phase angle δ suffers only slow variations, then the following approximate inequality holds

$$\cos\delta_{k+1}+\cos\delta_{k-1}\approx 2\cos\delta_k -\sin(\delta_k)(\delta_{k+1}+\delta_{k-1}-2\delta_k)\ . \tag{3.15}$$

Inserting this result into Eq. (3.14), and making use of Eq. (3.11) we have

$$b\sin(\delta_k)(\delta_{k+1}+\delta_{k-1}-2\delta_k) -A_0^2(\cos^3\delta_k-\cos\delta_k)=0\ . \tag{3.16}$$

After replacing the finite differences in Eq. (3.16) with the appropriate derivative, and utilizing some simple trigonometric identities we are left with the following nonlinear differential equation:

$$b\frac{d^2\delta}{dk^2}-\frac{cA_0^2}{2}\sin(2\delta)=0\ . \tag{3.17}$$

This equation supports a "sine-Gordon kink," in which the phase shift δ changes continuously from 0 to π. The characteristic distance, ξ, over which the phase shift suffers a substantial change—measured in units of the spacing between the pendulums—is given by

$$\xi=\sqrt{2b/cA_0^2}\propto(a+2b)^{-1/2}\ . \tag{3.18}$$

The assumption that the upper cutoff mode is just beyond the threshold of dynamical stability is consistent with a slow variation in the spatial phase shift.

IV. ANOTHER APPROACH: THE KINK

There is a way to introduce the approximation of a slowly varying envelope that allows one to extend the domain-wall configuration beyond the sine-Gordon kink. We begin by deriving a generalized equation for steady-state configurations in which amplitudes alternate between two sets of values as the site index changes from even to odd. Recalling our fundamental equation for amplitudes.

$$aA_i-b(A_{i+1}+A_{i-1})-cA_i^3=0\ , \tag{3.3}$$

we note that we can solve it for the amplitude of the central oscillator in terms of its two neighbors:

$$A_i=f(A_{i+1}+A_{i-1})\ . \tag{4.1}$$

An explicit form for the function f can be calculated explicitly, as Eq. (3.3) is a cubic equation. Using Eq. (4.1) to express A_{i+1} in terms of A_{i+2} and A_i, and similarly for A_{i-1}, we obtain the following equation coupling the amplitudes of oscillators on neighboring even- or odd-numbered sites

$$aA_i-b[f(A_{i+2}+A_i)+f(A_{i-2}+A_i)]-cA_i^3=0\ . \tag{4.2}$$

Now we imagine that A_{j+2} is close in value to A_j for every site index j. This allows us to perform a Taylor series expansion in Eq. (4.2). Replacing the discrete indexed variable A_i by $x(l)$, where l varies continuously, and assuming that $x(l+2)\approx x(l)$, Eq. (4.2) is replaced by

$$ax(l)-b\left[f\left[2x(l)+2\frac{dx}{dl}+2\frac{d^2x}{dl^2}+\cdots\right] +f\left[2x(l)-2\frac{dx}{dl}+2\frac{d^2x}{dl^2}+\cdots\right]\right]-cx(l)^3=0\ . \tag{4.3}$$

Expanding in the derivatives, and keeping second- and lower-order derivatives of $x(l)$, we are left with

$$ax(l)-2bf(2x(l))-4bf'(2x(l))\frac{d^2x}{dl^2} -4bf''(2x(l))\left[\frac{dx}{dl}\right]^2-c[x(l)]^3=0\ . \tag{4.4}$$

To further reduce the equation we choose $f(2x)$ as the variable whose l-dependence is to be sought. Given Eq. (4.1), we can obtain $x(l)$ in terms of f as follows

$$x(f(l))=\frac{af(l)-cf(l)^3}{2b}\ . \tag{4.5}$$

Then, using

$$\frac{d^2f}{dx^2}=-\left[\frac{df}{dx}\right]^3\frac{d^2x}{df^2}\ , \tag{4.6}$$

and

$$\frac{d^2x}{dl^2}=\left[\frac{df}{dl}\right]^2\frac{d^2x}{df^2}+\frac{dx}{df}\frac{d^2f}{dl^2}\ , \tag{4.7}$$

we arrive at the following equation

$$ax(f(l))-2bf(l)-c[x(f(l))]^3$$

$$-\left[b\Big/\frac{dx}{df}\right]\frac{d}{df}\left[\frac{dx}{df}\left[\frac{df}{dl}\right]^2\right]=0\ . \tag{4.8}$$

Equation (4.8) can be solved by quadratures. Its first integral is immediate:

$$b\frac{dx}{df}\left[\frac{df}{dl}\right]^2=\int^f\{ax(f')-2bf'$$

$$-c[x(f')]^3\}\frac{dx}{df'}df'+C\ . \tag{4.9}$$

Because x is a cubic in f, the integration is over a polynomial and can be carried out explicitly. The constant of integration on the right-hand side above guarantees that boundary conditions are met. In this case, the constant ensures that the function $f(l)$ approaches the appropriate asymptotic limit as $l\rightarrow\pm\infty$.

One further integration yields $f(l)$ as a function of l. Unfortunately, it is not possible to express the result of the final integration in terms of tabulated functions, as the integrand contains the square root of a ninth-order polynomial. However, it can be verified that when $a+2b$ is positive and small the solution is close to the sine-Gordon kink derived above. This is because, according to Eq. (4.5), $x(f)\approx -f$. Substitution into Eq. (4.9) leads to the solution for $f(l)$ as the ϕ^4 kink, which has an amplitude variation equivalent to the sine-Gordon kink.

As the quantity $a+2b$ increases so that the upper cutoff mode is well beyond threshold, the shape of the domain wall departs further and further from that of the simple kink. In fact, when the parameter a becomes positive, the assumption of a slowly varying envelope ceases to be valid. This is because the derivative df/dx diverges in the region containing the kink. The expression for $f(l)$ obtained by integrating Eq. (4.9) becomes singular when this occurs, in that the derivative df/dl is infinite. It is then necessary to abandon the slowly-varying-envelope approximation and utilize a method that recognizes the fact that the amplitudes of the pendulums' swings are discrete quantities as a function of location along the lattice. The replacement of a continuous by a discrete description will take place at some point in the vicinity of the region of most rapid variation of the amplitudes. There is no prescription that sets the exact location at which one matches the continuous with the discrete method, but a bit of inspection provides a likely point, at which one can verify that the domain wall is reproduced to a reasonable accuracy, at least in some parameter regimes. The rationale for the choice of a matching point follows from the structure of the curve giving the quantity x as a function of f. This curve is displayed in Fig. 1.

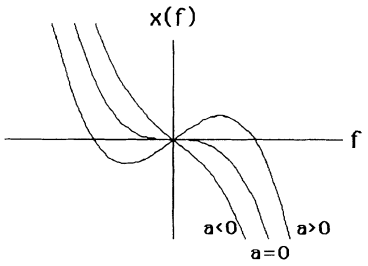

FIG. 1. Plot of the function $x(f)$ in the parameter ranges $a<0$, $a=0$, $a>0$. Note that when $a>0$, x is a nonmonotonic function of f.

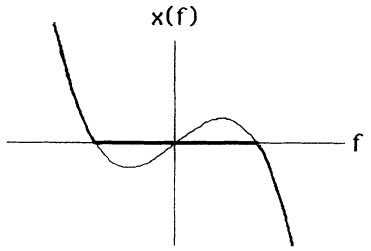

FIG. 2. Indicating how one bypasses the nonmonotonic region in the phase-shift kink when the parameter a is greater than zero.

Note that the function $x(f)$ is nonmonotonic when $a>0$, which means that f as a function of x is not single valued in this regime. The condition $a=0$ corresponds to the threshold of stability for the parametrically excited midband mode. This mode can also be characterized in terms of its periodicity on the lattice as a "$\lambda=4$" mode, where λ is the mode's wavelength in units of the lattice spacing. When $a<0$ the mode is not dynamically stable, and when $a>0$ it is.

On way to obtain a shape for the interface when $a>0$ is to apply the slowly-varying-envelope approximation in the range $\sqrt{(a+2b)/c}>|f|>\sqrt{a/c}$. This range encompasses the limit $l=\infty$, which corresponds to $f=\sqrt{(a+2b)/c}$, and extends to the point at which $x(f)=0$. One then extrapolates through a central point, which we identify with an $x(l=0)=0$, to the curve that is the inverted mirror image of slowly-varying-envelope approximation result on the other side of $l=0$.

Note that this method is equivalent to bypassing the nonmonotonic portion of the curve in Fig. 1 as illustrated in Fig. 2 (with the proviso that there is an isolated point in the center of the transition region). This is reminiscent of the Maxwell construction in the van der Waals theory of the gas-liquid system. In this light, it is not inappropriate to think of the domain wall as being the locus of an abrupt, or "first-order" shift in the lattice's configuration.

V. THE $\lambda=2$–$\lambda=4$ INTERFACE

Now to the interesting case. Experiments have established that modes with two different fundamental periodi-

cities can coexist in the pendulum lattice [3]. The local stability of this coexistence seems to be a consequence of the discrete spatial structure of the system. While there is no firm theoretical foundation for this conjecture its plausibility will be established in Sec. VII. We will now devise a method that allows for the application of the slowly-varying-envelope approximation to the case of the region separating an upper cutoff and a midband mode. The key to this approach is the observation that in both the $\lambda=2$ and the $\lambda=4$ modes the amplitude repeated every four lattice sites. In other words, four is the *least common multiple* of the spatial periodicities of the two coexisting modes. We will use this fact to extend the approach of the above section to the case at hand. In principle, the method utilized ought to be applicable to cases in which modes of arbitrary periodicities coexist.

In the remainder of this section, we will develop the slowly-varying-envelope approximation, explore the limits of its applicability, and briefly describe the numerical determination of the amplitudes in the core of the region in which the transition between the $\lambda=2$ and $\lambda=4$ modes takes place.

We start by noting that one can utilize Eq. (4.2) to construct an equation in which the amplitude at every *fourth* site enters. One accomplishes this by taking advantage of the fact that Eq. (4.2),

$$aA_i-b[f(A_{i+2}+A_i)+f(A_{i-2}+A_i)]-cA_i^3=0\ , \quad (4.2)$$

allows one, in principle, to solve for A_i in terms of A_{i+2} and A_{i-2}:

$$A_i=g(A_{i+2},A_{i-2})\ . \quad (5.1)$$

Substituting this into Eq. (4.2) one obtains the equation

$$aA_i-b[f(g(A_{i+4},A_i)+A_i)+f(g(A_{i-4},A_i)+A_i)]-cA_i^3=0\ , \quad (5.2)$$

where we have used the fact that the function g is symmetric in its two arguments. Now, we assume that $A_{j+4}=A_j$, and perform a gradient expansion in Eq. (5.2). If we replace A_i by $x(l)$, where, as in Sec. IV, l is a continuous variable, then

$$A_{j+4}\equiv x(l+4)\approx x(l)+4\frac{dx}{dl}+\tfrac{1}{2}(4)^2\frac{d^2x}{dl^2}+\cdots$$

and if we retain all terms of up to second order in the displacement $\delta\equiv 4$, Eq. (5.2) becomes

$$ax(l)-2bf[g(x(l),x(l))+x(l)]-c[x(1)]^2-b\delta^2\left[f'g_1\frac{d^2x}{dl^2}+f'g_2\left[\frac{dx}{dl}\right]^2+f''\left[\frac{dx}{dl}\right]^2\right]=0\ . \quad (5.3)$$

In the above equation we have introduced the following definitions:

$$f'=\frac{df(x)}{dx},\quad f''\frac{d^2f(x)}{dx^2}\ ,\qquad g_1=\frac{\partial g(x,y)}{\partial x},\quad g_2=\frac{\partial 2g(x,y)}{\partial x^2}\ . \quad (5.4)$$

We now choose the function $g(x,x)$ as the independent variable. The argument of f' is the same as the argument of the function f as it first appears in Eq. (5.3), while g_1 and g_2 have both arguments equal to $x(l)$. the reduction of Eq. (5.3) to a form that parallels Eq. (4.8) necessitates a few steps, which are relegated to the Appendix. The end result is the equation

$$ax(g)-2bf(g)-c[x(g)]^3-\frac{Bf'}{4\frac{dx}{dg}}\frac{d}{dg}\left[\frac{dx}{dg}\left[\frac{dg}{dl}\right]^2\right]=0\ . \quad (5.5)$$

In Eq. (5.5), the quantity B is equal to $b\delta^2$ and the functions $x(g)$ and $f(g)$ are defined in the Appendix. The quantity f' is as defined in (5.4), expressed as a function of g.

The steps leading to the solution of Eq. (5.5) are straightforward. Multiplying by the factor $(4\,dx/dg)/Bf'$) and integrating with respect to g:

$$\frac{dx}{dg}\left[\frac{dg}{dl}\right]^2=4\int_{g_0}^{g}\frac{ax(g')-2bf(g')-c[x(g')]^3}{Bf'(g')}\frac{dx}{dg'}dg'\ . \quad (5.6)$$

One further integration yields g as a function of l. A complicating feature of the solution obtained in this way arises from the fact that the derivative dx/dg passes through zero in the region of the domain wall. This means that there is no entirely smooth interpolation between the two regimes. However, it is possible to join two solutions of the form embodied in Eq. (5.6), one in the wavelength-two regime and the other in the wavelength-four regime. The resulting domain wall is continuous, but has a singularity in the form of an infinite first derivative. Nevertheless, as we will see, this continuous domain wall reproduces the structure of the transition region observed in the actual pendulum lattice, and in simulations of such a lattice. The singularity of the slowly-varying-envelope approximation does not seem to signal a fatal pathology in the method as applied to this problem.

VI. NUMERICAL CALCULATIONS AND COMPARISON WITH DATA

In order to assess the quantitative reliability of the solutions obtained via the method described in the previous section, we compare the interface profile as calculated with the use of the slowly-varying-envelope approximation with data generated by numerical integration of Eq. (2.1). Table I contains values for the displacements from equilibrium of the oscillators in a 50-component lattice containing a $\lambda=2$–$\lambda=4$ interface [10]. The values listed represent a "snapshot" of the lattice, the snapshot having been taken when the displacements were at their greatest values. The accuracy of these values are limited because of two features of the method by which they were obtained. First, the point in time at which the oscillator displacements are largest was determined by observation of an animated display, rather than by a more pre-

TABLE I. The displacements of the oscillators in a 50-oscillator array at the instant at which those displacements are maximum. See the comments in the first paragraph of Sec. VI for a discussion of the reliability of the data. This data is the result of a numerical integration of the equation of motion Eq. (2.1).

Oscillator index	Amplitude	Oscillator index	Amplitude
0	−0.622 787	21	0.035 303
1	0.622 787	22	−0.365 355
2	−0.622 787	23	−0.010 449
3	0.622 787	24	0.356 555
4	−0.622 787	25	0.003 439
5	0.622 787	26	−0.354 037
6	−0.622 787	27	−0.001 353
7	0.622 787	28	0.353 315
8	−0.622 787	29	0.000 675
9	0.611 788	30	−0.353 109
10	−0.622 788	31	−0.000 404
11	0.622 788	32	0.353 052
12	−0.622 789	33	0.000 265
13	0.622 788	34	−0.353 037
14	−0.622 764	35	−0.00 018
15	0.622 538	36	0.353 033
16	−0.620 714	37	0.000 123
17	0.606 546	38	−0.353 033
18	−0.500 338	39	0.000 084
19	−0.133 588	40	0.353 034
20	0.396 509	41	0.000 056
42	−0.035 3034	46	−0.353 035
43	−0.000 036	47	−0.000 006
44	0.353 034	48	0.353 035
45	0.000 020	49	−0.000 006

cise numerical analysis of the data. Second, the oscillators do not achieve maximum excursions from equilibrium simultaneously. There are small, but nonnegligible differences in the phases of the oscillators so a snapshot cannot yield values for the amplitudes of all oscillators. This has been noted experimentally [11], and it can be understood analytically [12]. Fortunately, for the configurations most directly relevant to the case at hand the differences between the phases do not exceed about 5°.

Figure 3 displays the displacements numerically. Oscillators farther out on either side propagate the patterns set by the closer-in oscillators. In other words, the $\lambda=2$ and 4 modes are well established in the regime displayed in Fig. 3.

The validity of the time-averaged equations underlying the slowly-varying-envelope approximation is tested by evaluating the left-hand side of Eq. (3.3), with coefficients adjusted as follows: $a=0.947$, $b=1$, $c=7.598$. The homogeneity of Eq. (3.3) allows us to set one of the above coefficients equal to 1, and that has been done. The coefficients a and c were then determined by fitting to the amplitudes of the $\lambda=2$ and 4 modes bracketing the domain wall. The results of this test are also displayed in Fig. 3. Deviations from zero are largest in the immediate vicinity of the domain wall, but, at their greatest, they do not exceed about 1%. This conforms with the limitations suggested by the phase differences and presents us with a bound on both the reliability of the data and the quality of the time-averaged equations.

Figure 4 contains a comparison of the data with the quantities $f(l)$, $g(l)$, and $x(l)$ as obtained from Eqs. (5.5), (5.6), (A1), and (A2). The fit to the data was accomplished by adjusting the horizontal scale and shifting the

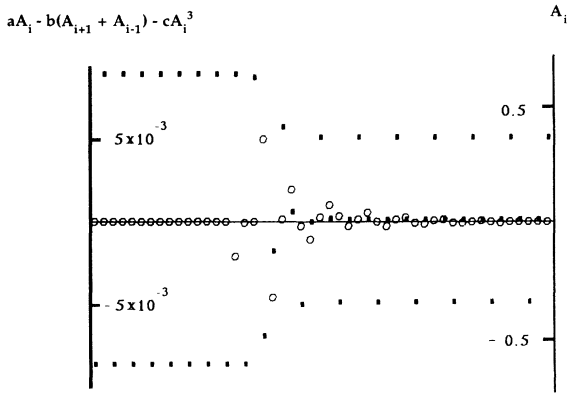

FIG. 3. The displacements of the oscillators in the 50-oscillator array at the instant at which those displacements are maximum. See the comments in the first paragraph of Sec. VI for a discussion of the reliability of the data. Also displayed are the numerical values of the right-hand side of Eq. (3.3), when the data for the displacements are utilized. The right-hand ordinate establishes the scale for the displacements, which appear as filled rectangles and the left-hand ordinate refers to the results for the left-hand side of Eq. (3.3), the values of which are displayed as open circles.

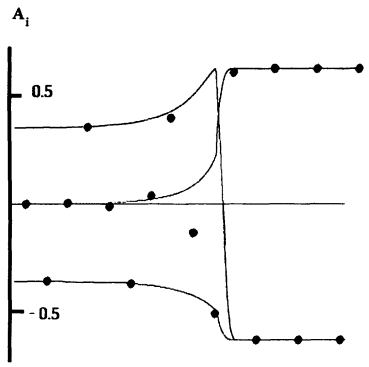

FIG. 4. Comparison of the displacements of the 17 oscillators closest to the $\lambda=2-4$ domain wall with the results for $g(l)$, $x(l)$, and $f(l)$ obtained from Eqs. (5.5), (5.6), (A1), and A2).

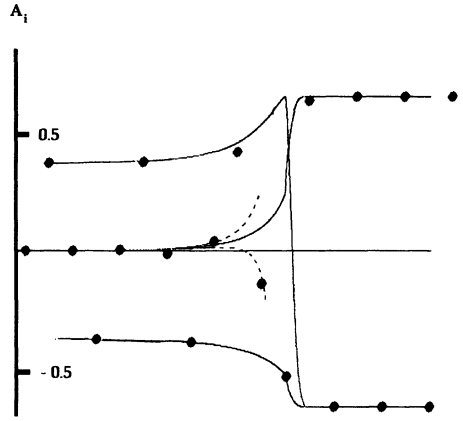

FIG. 5. Comparison of the displacements of the 17 oscillators closest to the $\lambda=2-4$ domain wall with the use of Eqs. (5.5), (5.6), (A1), and (A2), and also Eq. (6.3), which approximates the differences between the behavior of the two sublattices $f_1(l)$ and $f_2(l)$.

horizontal axis. Note that the comparison is restricted to the 17 oscillators in the immediate vicinity of the domain wall. The function $g(l)$ as depicted on the plot interpolates smoothly between two negative values, while the function $x(l)$ rapidly varies from a positive value on one side of the domain wall to a negative value on the other side. The functions $g(l)$ and $x(l)$ approach the same asymptote in the region of the $\lambda=2$ mode and have equal and opposite values in the $\lambda=4$ mode. The function $f(l)$ interpolates between and asymptotic value of zero in the $\lambda=4$ regime and a value equal and opposite to $g(l)$ and $x(l)$ in the $\lambda=2$ regime. As the figure clearly indicates, the slowly-varying-envelope approximation replicates the amplitudes on the two sublattices labeled $x(l)$ and $g(l)$, but it is *not* satisfactory for the two sublattices corresponding to the function $f(l)$. This probably arises from the attempt to encompass the amplitudes on two separated sublattices by a single, continuous, function.

We may attempt to take into account the difference between the "f sublattices" by noting that one of them consists of oscillators flanked on the left by a "g-sublattice" oscillator and on the right by an "x-sublattice" oscillator, while on the other f sublattice the locations of the two neighboring oscillators are reversed. We can take this into account by rewriting Eq. (A2) as two equations, each appropriate to one of the two f sublattices, i.e.,

$$af_1(l)-c[f_l(l)]^3=x(l+\delta)+g(l-\delta) \tag{6.1}$$

and

$$af_2(l)-c[f_2(l)]^3=x(l-\delta)+g(l+\delta)\ . \tag{6.2}$$

If the derivations from $f(l)$ induced by the difference between the right-hand sides of Eqs. (6.1) and (6.2) and the right-hand side of Eq. (A2) are small, then a low-order Taylor expansion suffices to calculate those differences. Writing $f_1(l)=f(l)+\Delta(l)$, $f_2(l)=f(l)-\Delta(l)$, we have

$$\Delta(l)=\frac{\delta\left[\dfrac{dx}{dl}-\dfrac{dg}{dl}\right]}{af(1)-3c[f(l)]^3}\ . \tag{6.3}$$

Figure 5 displays a comparison between the data and the corrected slowly-varying-envelope approximation. The improved envelope functions, $f_1(l)$ and $f_2(l)$, for the two sublattices are displayed as broken curves. The agreement with data is, obviously, greatly improved. This comparison is not entirely honest, however, in that the quantity δ has been adjusted to yield a best fit, rather than to achieve consistency with the horizontal scale. Nevertheless, the trends are clearly in the right direction.

VII. CONCLUSION

While the interface between $\lambda=2$ and a $\lambda=4$ mode differs from the localized structures previously observed in the linear array of oscillators, we have seen that the approximation of a slowly varying envelope, suitably modified, provides the basis for an acceptable quantitative model of its structure. In light of this, a similarly constructed model ought to describe the transition region between coexisting modes with less compatible periods. Such coexistence has been observed in simulations of the oscillator array [13]. The derivation of the more general model will likely prove more difficult, and the equations corresponding to Eq. (5.5) more cumbersome, but the form of the equation will probably allow for the kind of numerical integration that was utilized to obtain solutions in the case at hand.

We now return, briefly, to two issues raised in the body of this paper. The first has to do with the dynamical stability of a state comprised of two coexisting modes. It is reasonable to assume that there is, in general, a dynamical "preference" for one of the modes, and—if it were possible—that the favored mode would invade the region occupied by the less-favored mode. Ultimately, this process leads to the elimination of less-favored mode. However, the most natural way for one mode to displace another is for the entire configuration to translate along the array. The modes as depicted in Figs. 3–5 are clearly in registry with the lattice, and such a translation would entail a disruption of this registry. Thus, spatial phase

locking most likely pins the interface and, as a result, guarantees its local stability. Of course, if the array were subject to stochastic perturbations the stability of the interface could not be taken for granted. Thus, it is not clear whether the kind of coexistence we have been discussing here will occur in charge-density-wave systems. This issue deserves further study.

The second point has to do with the fact that the envelope has an infinite first derivative in the transition region, as noted in Sec. V. This singularity clearly violates the rationale for the gradient expansion leading to Eq. (5.3). However, it also widens the range of applicability of the slowly-varying-envelope approximation. Because of this singularity, the slowly-varying-envelope approximation predicts a transition region between two coexisting modes without requiring any degeneracy between the modes. To see that this is true, and in what way, imagine the situation as it would exist if the derivative dx/dg were everywhere finite and never changed sign. Then Eq. (5.5) could be analyzed in terms of the standard dynamical analogy applied to, for instance, the equation obeyed by the standard, hyperbolic tangent, kink. This interface is governed by the same equation as controls the motion of a ball balanced almost at equilibrium on top of one of two peaks, which rolls over to the second peak, approaching the top where it is again almost at equilibrium. Clearly, the two peaks must have the same elevation. The case at hand has similar dynamical analogy. The existence of a solution corresponding to a transition region between two modes that extend arbitrarily far out from the interfacial region thus entails a degeneracy condition. This is the global condition derived by Denardo, *et al* [7]. On the other hand, the singularity provides a point at which two nominally incompatible solutions can be "stitched" together.

ACKNOWLEDGMENTS

It is a pleasure to acknowledge discussions with Professor Seth Putterman, William Wright, Ritva Löfstedt, Bradley Barber, Alan Greenfield, Robert Hiller, and other members of the Putterman group. The author is especially indebted to Professor Putterman for suggestions that have had a fundamental impact on the work reported in this paper. Thanks are also due to W. Wright for equally important comments, and we express our gratitude to W. Wright for supplying the unpublished data with which the theory was compared.

APPENDIX

To reduce Eq. (5.3) to the compact form of Eq. (5.5), we need to make use of a number of relations, easily derivable from the definitions of the functions f and g. First,

$$\frac{ag-cg^3}{2b}=f(x+g) \tag{A1}$$

and

$$\frac{af(x+g)-c[f(x+g)]^2}{b}=x+g\ . \tag{A2}$$

These two relations enable us to express both $x(g)$ and $f(g+x)$ as a function of g. Note that the dependent variable x will be a ninth-order polynomial in g. Now, because the function $g(x,x)$ is symmetric in its two arguments, the partial derivative $g_1(x,x)$ is equal to half the total derivative $dg(x,x)/dx$. To obtain a result for $g_2(x,x)$, we note that the following equation defines the function $g(x,y)$

$$\frac{ag-cg^3}{b}\equiv A(g)=f(g+x)+f(g+y)\ . \tag{A3}$$

Then,

$$g_1A'(g)=f'(g+x)(1+g_1)+f'(g+y)g_1\ , \tag{A4}$$

so,

$$g_1(x+y)=\frac{f'(g+x)}{A'(g)-f'(g+x)-f'(g+y)}\ . \tag{A5}$$

Setting $x=y$,

$$g_1(x,x)=\frac{f'(g+x)}{A'(g)-2f'(g+x)}=\frac{1}{2}\frac{dg}{dx}\ . \tag{A6}$$

Taking an additional derivative of Eq. (A5) with respect to x, and then setting $x=y$ we obtain

$$g_2(x,x)=\frac{[A'(g)-2f'(g+x)]f''(g+x)[1+g_1(x,x)]}{[A'(g)-2f'(g+x)]^2}-\frac{f'(g+x)\{[A''(g)-2f''(g+x)]g_1(x,x)-f''(g+x)\}}{[A'(g)-2f'(g+x)]^2}\ . \tag{A7}$$

If we now take a derivative of dg/dx and make use the right-hand side of Eq. (A6) we obtain

$$\frac{d^2g}{dx^2}=\frac{2f''(g+x)\left[1+\frac{dg}{dx}\right]}{A'(g)-2f'(g+x)}-\frac{2f'(g+x)\left[[A''(g)-2f''(g+x)]\frac{dg}{dx}-2f''(g+x)\right]}{[A'(g)-2f'(g+x)]^2}\ . \tag{A8}$$

Combining Eqs. (A6), (A7), and (A8), we are left with the following relationship between $g_2(x,x)$ and the first and second derivatives of $g(x,x)$

$$g_2(x,x)=\frac{1}{4}\frac{d^2g}{dx^2}-\frac{1}{4}\frac{f''(g+x)}{f'(g+x)}\left[\frac{dg}{dx}\right]^2. \tag{A9}$$

The terms in Eq. (5.3) containing the partial derivatives $g_1(x,x)$ and $g_2(x,x)$ then reduce as follows:

$$f'(g+x)g_2(x,x)+f''(g+x)[g_2(x,x)]^2 = \frac{f'(g+x)}{4}\frac{d^2g}{dx^2}, \tag{A10}$$

and Eq. (5.5) follows immediately.

[1] R. Keolian, L. Turkevich, S. Putterman, I. Rudnick, and J. Rudnick, Phys. Rev. Lett. **47**, 1133 (1981).

[2] B. Denardo, Ph.D thesis, University of California, Los Angeles, CA, 1990.

[3] B. Denardo, B. Galvin, A. Greenfield, A. Larraza, S. Putterman, and W. Wright, Phys. Rev. Lett. **68**, 1730 (1992).

[4] A. Greenfield, W. Wright, and S. Putterman, Phys. Lett. A **185**, 321 (1994).

[5] J. D. van der Waals, Z. Phys. Chem. **13**, 657 (1894).

[6] See, for example, R. K. Dodd, J. C. Eilbeck, J. D. Gibbon, and H. C. Morris, *Solitons and Nonlinear Wave Equations* (Academic, New York, 1982).

[7] B. Denardo, A. Larraza, S. Putterman, and P. Roberts, Phys. Rev. Lett. **69**, 597 (1992). See, also, P. Roberts and S. Putterman, Proc. R. Soc. **440**, 135 (1993).

[8] See, for example, J. Moser, *Stable and Random Motions in Dynamical Systems* (Princeton University Press, Princeton; NJ, 1973).

[9] P. Bak, Rep. Prog. Phys. **45**, 587 (1982).

[10] This data was generated by William Wright.

[11] B. Denardo and W. Wright (unpublished).

[12] J. Rudnick (unpublished).

[13] W. Wright and S. Putterman (private communication).